Optimal paths in strong and weak disorder: A unified approach

Sergey V. Buldyrev,[1,2] Shlomo Havlin,[3,2] and H. Eugene Stanley[2]

[1]*Department of Physics, Yeshiva University, 500 West 185th Street, New York, New York 10033, USA*
[2]*Center for Polymer Studies and Department of Physics, Boston University, Boston, Massachusetts 02215, USA*
[3]*Minerva Center and Department of Physics, Bar-Ilan University, 52900 Ramat-Gan, Israel*
(Received 23 August 2005; published 28 March 2006)

We present a unified scaling theory for the optimal path connecting opposite edges of a disordered lattice of size L. Each bond of the lattice is assigned a cost $\exp(ar)$, where r is a uniformly distributed random variable and a is disorder strength. The optimal path minimizes the sum of the costs of the bonds along the path. We argue that for $L \gg a^\nu$, where ν is the correlation exponent of percolation, the path becomes equivalent to a directed polymer on an effective lattice consisting of blobs of size $\xi = a^\nu$. It is self-affined and characterized by the roughness exponent of directed polymers χ. For $L \ll a^\nu$, or on the length scales below the blob size ξ, the path behaves as an optimal path in the strong disorder limit. It has a self-similar fractal shape with fractal dimension d_{opt}. We derived the scaling relations for the length of the path, its transversal displacement, the average cost and its fluctuation. We test our scaling theoretical predictions by numerical simulations on a square lattice.

The statistical properties of optimal paths in a disordered energy landscape have been studied extensively in recent years [1–16]. Path properties are relevant to many optimization problems, including folding of proteins, spin glasses and the well-known traveling salesman problem [17]. Several studies considered the optimal paths in the strong disorder limit, where a single site or bond weight dominates the weight of the whole path, and found that the length ℓ of the optimal path scales with distance r as $r^{d_{\mathrm{opt}}}$, where $d_{\mathrm{opt}} = 1.22 \pm 0.02$ in $d=2$ and $d_{\mathrm{opt}} = 1.43 \pm 0.03$ in $d=3$ [6,10]. For weak disorder, the optimal path between the opposite edges of the lattice is assumed to belong to the directed polymer universality class characterized by a self-affined shape of the path with roughness exponent χ [5,9]. The total cost of the optimal path in weak disorder increases linearly with the distance L between the edges; however, its root mean square fluctuation increases as L^ω, with $\omega < 1/2$. The exponents $\chi = \beta/\alpha$ and $\omega = \beta$ are related to the exponents of the Kardar, Parisi, and Zhang (KPZ) equation α and β in $d+1$ dimensions [2]. For $d=1$, the values of $\alpha = 1/2$ and $\beta = 1/3$ are known exactly [4,5].

The weak disorder problem characterizes the behavior of a long polymer chain of total length N which crosses a slab of width $L \ll N$ (Fig. 1). The slab is filled with a disordered media which repulses the monomers with potential $E(\mathbf{r}_i) > 0$ which is a random function of the coordinates $\mathbf{r}_i$ of the monomers. The media outside the slab does not interact with the polymer. The ends of the polymer cannot penetrate through the membrane of the slab. In the limit of zero temperature, the polymer minimizes its total potential energy $E = \Sigma_{i=1}^{\ell} E(\mathbf{r}_i)$, where ℓ is the number of monomers inside the slab. If the distribution of $E(\mathbf{r})$ becomes very broad and non-uniform, the sum of the potential energies is dominated by the largest potential energy, and we have a transition to strong disorder. Here we present a unified scaling approach for the behavior of the polymer inside the slab for both weak and strong disorder and for the crossover between these two

regimes that is supported by numerical simulations on a square lattice.

We consider lattices of linear size L in which each bond is assigned a cost $E_i = \exp(ar_i)$ where r_i is uniformly distributed between 0 and 1. The optimal path minimizes the total cost of its bonds between the two edges of the lattice. In the strong disorder limit, when $a \to \infty$, the cost of the path is dominated by the largest cost $r_{i,\mathrm{max}}$. Thus the optimal path must minimize $r_{i,\mathrm{max}}$, hence all bonds of the optimal path must belong to the backbone of the percolation cluster [18,19] first connecting the opposite edges of the lattice as we include into it the bonds with larger and larger r_i. By construction, the fraction of bonds p_1 at which percolation
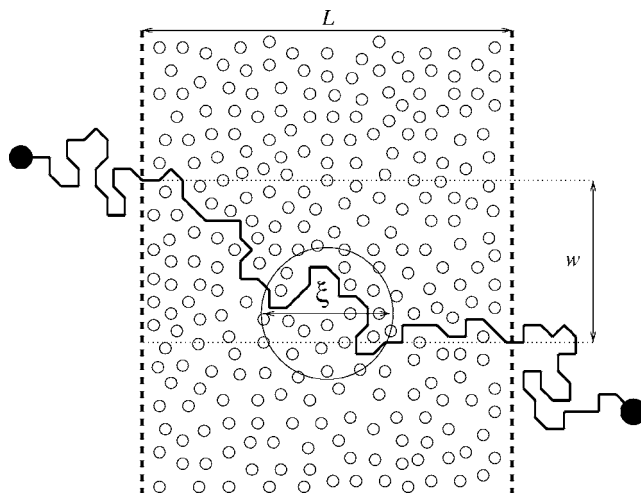

FIG. 1. The polymer penetrating through the slab of width L is characterized by the total number of monomers inside the slab ℓ, their potential energy E, and the transversal displacement w between the monomers at the opposite sides of the slab. A blob of percolation correlation length ξ, within which the polymer has a self-similar shape with fractal dimension d_{opt}, is represented schematically by a large circle.

occurs is equal to the minimum of $r_{i,\max}$ among all possible paths connecting the opposite edges of the lattice [12]. For finite lattices of linear size L, the value of p_1 for which percolation first occurs is distributed as a narrow distribution with mean p_c, and standard deviation $\sigma_0 = C/L^{1/\nu}$, where C is some constant of the order of unity [19]. Here we assume that the narrow distribution is Gaussian and we support its numerical simulations. The largest weight on the optimal path is thus equal to $\exp(p_1 a)$. The distribution of the total cost $E \approx \exp(p_1 a)$ of the optimal path is thus a log-normal distribution

$$P(E) = \frac{1}{\sqrt{2\pi}\sigma_0 a E} e^{[\ln(E) - ap_c]^2/2a^2\sigma_0^2}, \tag{1}$$

with mean

$$\mu = \exp\left(ap_c + \frac{(a\sigma_0)^2}{2}\right) \tag{2}$$

and standard deviation

$$\sigma = \mu\sqrt{\exp[(a\sigma_0)^2] - 1}. \tag{3}$$

The crossover from strong to weak disorder starts to occur when the optimal path may not necessarily go through the bond with the cost $\exp(ap_1)$ but may prefer to go through the bond with the larger cost $\exp(ap_2)$, where $p_2 > p_1$ is the fraction of bonds at which percolation would occur, provided that the bond p_1 has been removed. These values p_1 and p_2 belong to the same Gaussian distribution of the percolation thresholds and hence their expected difference $\langle p_2 - p_1 \rangle = C_1\sigma_0$ where C_1 is a constant of the order of unity. The next to the best path in strong disorder limit may become the best for finite disorder a if $a(p_2 - p_1)$ is a small number of the order of unity and hence $a\sigma_0 \sim a/L^{1/\nu}$ must be of the order of unity when the deviation from the strong disorder behavior can be observed. (See also Refs. [14,15] for the analogous conductance problem and Refs. [13,16] for random networks.) Our numerical simulations on a square lattice confirm this theoretical prediction. Figure 2 shows the distribution of the total cost for large $a = 32$, and several small values of L. One can see that when $a/L^{1/\nu} \gtrsim 3.8$, the distribution of the total cost can be well approximated by a log-normal distribution with mean ap_c and variance $a\sigma_0 \approx 0.36a/L^{1/\nu}$, where $\nu = 4/3$ [18,19] in two dimensions. However, for $a/L^{1/\nu} \approx 2.3$ we already see a significant departure of the mean value of the total cost from the percolation predictions.

The above considerations suggest that we can introduce a blob of correlation length $\xi = a^\nu$, within which a path behaves as in the strong disorder limit, while for length scales much larger than ξ it behaves as a directed polymer of

$$n_b = L/\xi = L/a^\nu \tag{4}$$

effective bonds of length ξ. For each bond the cost is distributed according to a relatively narrow log-normal distribution (1) with a scaling parameter $\sigma^* \equiv a\sigma_0 \sim 1$, which determines mean μ, and standard deviation σ according to Eqs. (2) and (3).

Next we study the distribution of the total cost E. For $L/a^\nu \gg 1$, we expect that the total cost E behaves as in the
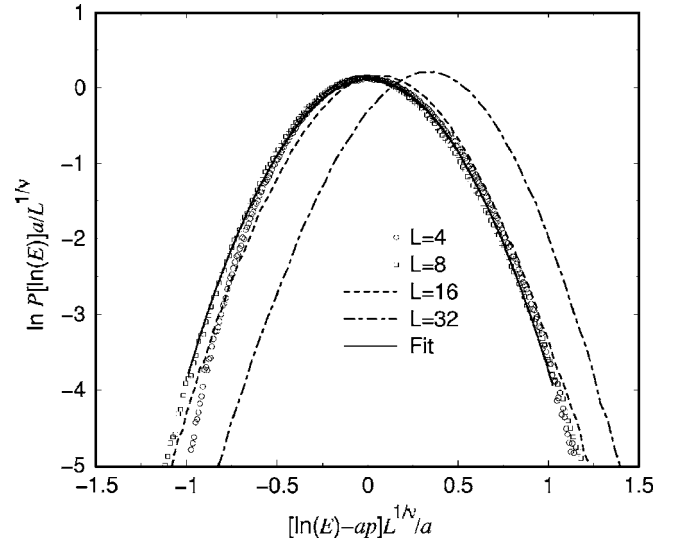

FIG. 2. Logarithm of the distribution of the logarithm of the total cost for $a = 32$ and several small L scaled by $a/L^{1/\nu}$. For very small L, the graphs are indeed log-normal distributions (1), which is demonstrated by the parabolic fit, giving $\sigma_0 = 0.36L^{-1/\nu}$. While for large $a/L^{1/\nu} \gtrsim 3.8$ ($L=4,8,16$), the distributions scale almost exactly as predicted by the percolation theory in the strong disorder limit; for smaller $a/L^{1/\nu} \approx 2.3$ ($L=32$), one can already see significant deviations from the percolation theory.

directed polymer problem. Due to global optimization, the values of the cost for each bond cannot be considered independent random variables, and thus their sum does not converge to a Gaussian distribution but converges to an asymmetric distribution,

$$P(E) = \sigma_E^{-1} P_D[(E - \langle E \rangle)/\sigma_E], \tag{5}$$

of the directed polymer problem with mean $\langle E \rangle$ and standard deviation σ_E. For large n_b, we expect that

$$\langle E \rangle/n_b \rightarrow \mu_\infty(\mu, \sigma) \tag{6}$$

and standard deviation

$$\sigma_E/n_b^\omega \rightarrow \sigma_\infty(\mu, \sigma), \tag{7}$$

where the limits $\mu_\infty(\mu, \sigma)$ and $\sigma_\infty(\mu, \sigma)$, are homogeneous functions of μ and σ of the first order, i.e., $\mu_\infty(\lambda\mu, \lambda\sigma) = \lambda\mu_\infty(\mu, \sigma)$ and $\sigma_\infty(\lambda\mu, \lambda\sigma) = \lambda\sigma_\infty(\mu, \sigma)$ for any $\lambda > 0$ [20]. Assuming $\lambda = \exp(a_p c)$, we find from Eqs. (2) and (3) that

$$\mu_\infty = \exp(ap_c)f_\mu(\sigma^*) \tag{8}$$

and

$$\sigma_\infty = \exp(ap_c)f_\sigma(\sigma^*), \tag{9}$$

where the functions $f_\mu(\sigma^*)$ and $f_\sigma(\sigma^*)$ with $\sigma^* \sim 1$ may have only weak dependence on a and must converge to some limits when $a \rightarrow \infty$. In the strong disorder limit $L/a^\nu < 1$, we expect

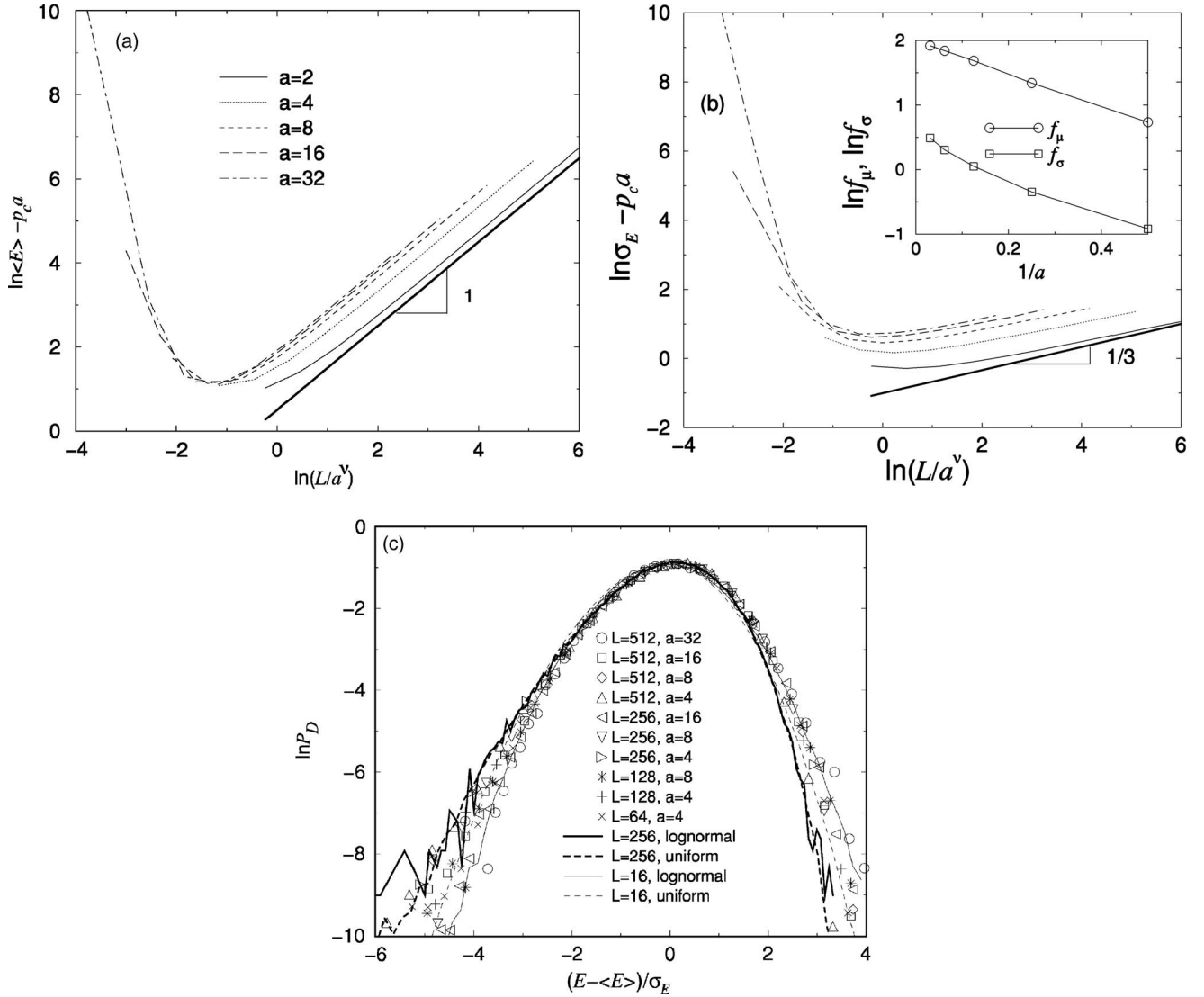$$\langle E \rangle \sim \exp(a^2\sigma^2/2) = \exp(Ca^2L^{-2/\nu}) \tag{10}$$

FIG. 3. (a) Double logarithmic plot of the scaled average total cost $\langle E \rangle$ versus the scaling variable L/a^ν. For $L/a^\nu < 1$, the total cost rapidly decreases with L, while for large L/a^ν the total cost increases proportionally to n_b with different proportionality coefficients $f_\mu(a)$, which can be found as the intercepts of the straight line fit with slope 1 (bold line) to the graphs for large L/a^ν. (b) Double logarithmic plot of the scaled standard deviation of the total cost versus scaling variable L/a^ν. For $L/a^\nu < 1$, the behavior is analogous to the behavior of the average cost. For large n_b, the slopes of the graphs approach asymptotic value $\omega = 1/3$ indicated by a bold straight line. The intercepts of the straight line fits gives the values of the coefficients $f_\sigma(a)$. Inset: the behavior of the coefficients $f_\mu(a)$ and $f_\sigma(a)$ found in part (a) and (b), as functions of $1/a$ indicate the convergence of their values for $a \to \infty$. (c) The scaled distribution of the total cost for various L and a for $n_b > 5$ in comparison to the distribution of the total cost for the uniform and log-normal distribution of the bond costs.

and

$$\sigma_E \sim \exp(a^2 \sigma_0^2 / 2) = \exp(Ca^2 L^{-2/\nu}) \quad (11)$$

to diverge as $L/a^\nu \to 0$.

To test the predictions of Eqs. (6)–(11), we plot the logarithm of the average cost $\langle E \rangle$ and its standard deviation σ_E versus the logarithm of L/a^ν [Figs. 3(a) and 3(b)] and find good agreement with Eqs. (6) and (7). Indeed, for $L/a^\nu \to \infty$, the graphs for $\langle E \rangle$ and σ_E become straight lines with slopes 1 and $\omega = 1/3$, respectively, and their intercepts $\ln \mu_\infty$ and $\ln \sigma_\infty$ converge for $a \to \infty$ to finite limiting values as indicated in the inset of Fig. 3(b). For $L/a^\nu \to 0$, we find divergence of $\langle E \rangle$ and σ_E as expected from Eqs. (10) and

(11). Figure 3(c) illustrates the convergence for $n_b \to \infty$ of the scaled distributions of the total cost to a universal function P_D defined in Eq. (5). In addition to the strong disorder distributions, we also plot the scaled distributions of the total costs for the uniform distribution and log-normal distribution of costs E_i of the individual bonds. These two distributions are obtained for a uniform distribution of E_i on the interval $[0, 1]$ and a log-normal distribution of $P(E_i) = (E_i \sqrt{2\pi})^{-1} \exp[\ln^2(E_i)/2]$ for $L=256$ and for $L=16$. We can see a relatively good convergence to the distribution of the same general shape with the left tail decaying slower than the right tail.

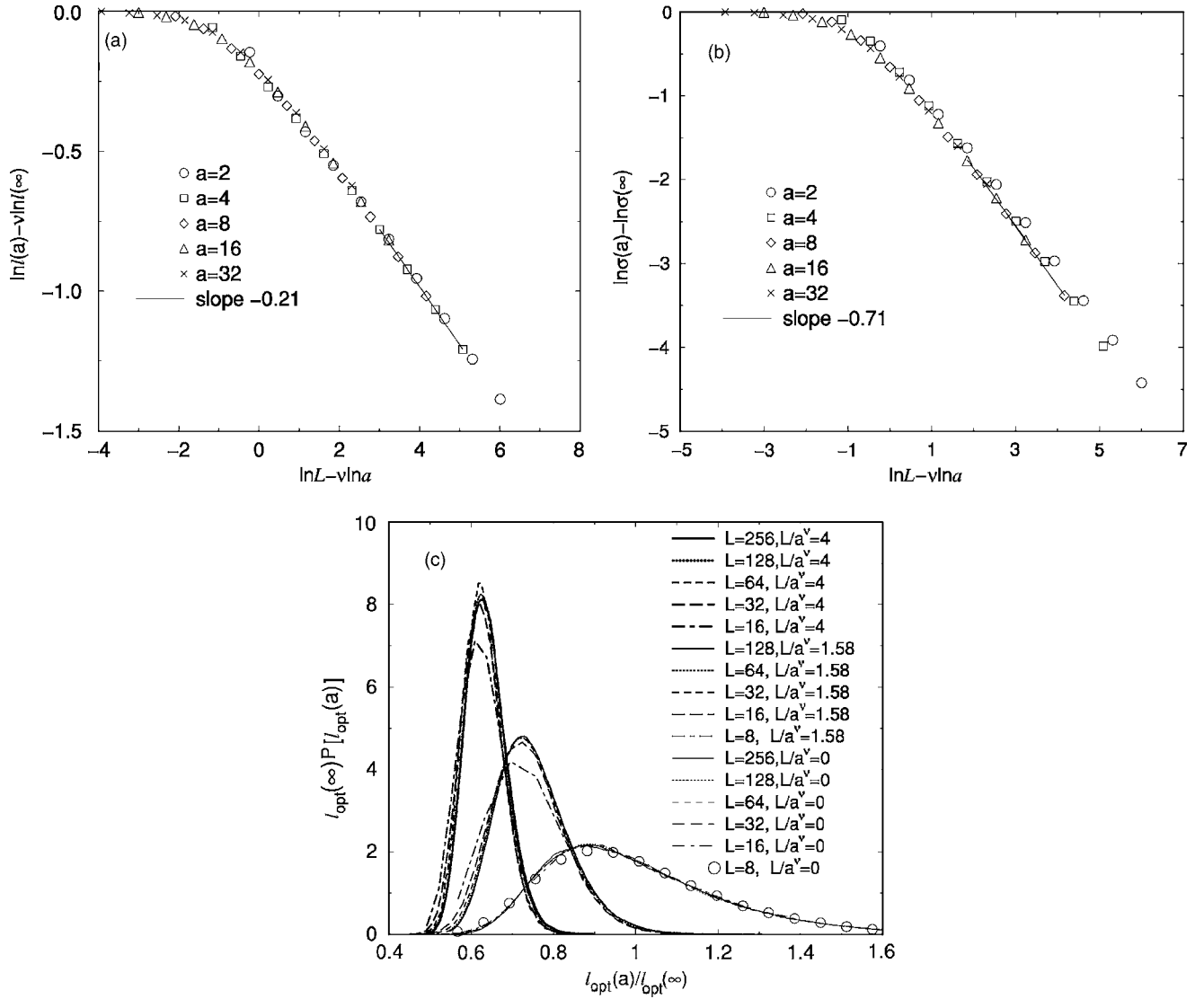Next we discuss the behavior of the optimal path length ℓ.

FIG. 4. (a) Double logarithmic plot of the scaled averaged path length $\ell(a)/\ell(\infty)$ for various values of a. The slope of the graph converges to $1-d_{\mathrm{opt}} \approx -0.2$ for large $n_b \equiv L/a^\nu$. (b) Double logarithmic plot of the scaled averaged path fluctuation $\sigma_\ell(a)/\sigma_\ell(\infty)$ for various values of a. The slope of the graph converges to $1/2-d_{\mathrm{opt}} \approx -0.7$ for large $n_b \equiv L/a^\nu$. (c) Scaled distributions of the optimal path for three different relative disorder strengths L/a^ν. The $L/a^\nu=0$ curves correspond to the distribution of optimal path in strong disorder ($a=\infty$).

The distribution of the optimal path length within a blob, ℓ_b, is a relatively narrow distribution with mean

$$\langle \ell_b \rangle \sim a^{\nu d_{\mathrm{opt}}} \tag{12}$$

and standard deviation

$$\sigma_{\ell_b} \sim a^{\nu d_{\mathrm{opt}}}. \tag{13}$$

If we assume that the lengths of the path within each blob are identically distributed independent random variables, the distribution of the total optimal path length ℓ must converge for large n_b to a Gaussian with mean

$$\langle \ell \rangle = n_b a^{\nu d_{\mathrm{opt}}} = L^{d_{\mathrm{opt}}} = n_b^{1-d_{\mathrm{opt}}} \tag{14}$$

and standard deviation

$$\sigma_\ell = \sigma_{\ell_b} \sqrt{n_b} = L^{d_{\mathrm{opt}}} n_b^{1/2-d_{\mathrm{opt}}}. \tag{15}$$

Figures 4(a) and 4(b) show good agreement with these theoretical predictions.

Thus, the distribution of the scaled optimal path length $x=\ell/L^{d_{\mathrm{opt}}}$ can be represented in a general scaling form: $P_\ell(x,n_b)$, where $n_b=1$ for $L \ll a^\nu$ and $n_b \sim L/a^\nu$ for $L \gg a^\nu$ [Fig. 4(c)]. To achieve better data collapse in Fig. 4, we use instead of $L^{d_{\mathrm{opt}}}$ the quantity $\ell(\infty)$, which is the length of the path in the strong disorder limit $a \rightarrow \infty$. For $L \gg 1$ the quantities asymptotically coincide $\ell(\infty) \sim L^{d_{\mathrm{opt}}}$. The mean and standard deviation of $P_\ell(x,n_b)$ decrease with n_b as $n_b^{1-d_{\mathrm{opt}}}$ and $n_b^{1/2-d_{\mathrm{opt}}}$, respectively [Figs. 4(a) and 4(b)] as given by Eqs. (14) and (15).

Analogously, we can explain the behavior of the transversal deviation w between the beginning and the end of the
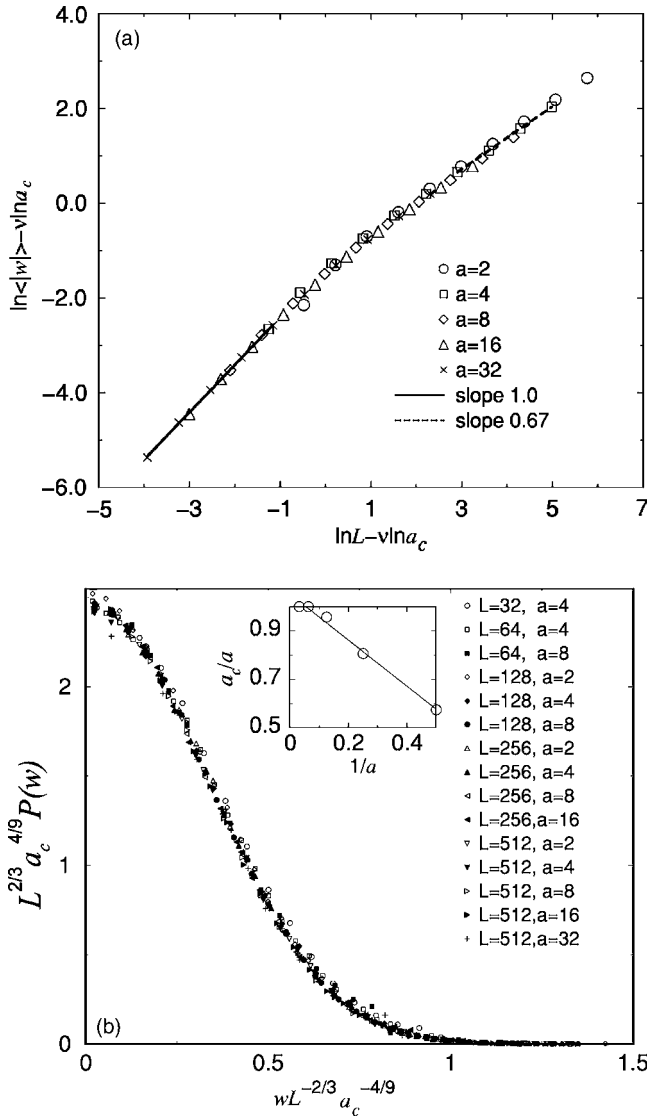
FIG. 5. (a) Double logarithmic plot of the scaled averaged transversal deviation of the path $\langle|w|\rangle/\xi=\langle|w|\rangle/a_c^\nu$ for various values of a versus scaled length $L/\xi=L/a_c^\nu$. The values of the correction coefficients a_c/a are presented in the insets of part (b). The slopes of the graphs change from 1 (solid line) for small $L/a_c^\nu<1$ to $\chi=2/3$ (dashed line) for large $L/a_c^\nu>1$. (b) Distributions of the scaled transversal deviation of the optimal path for several values of a and L. The distributions converge to a Gaussian distribution for large L/a^ν. Inset: the behavior of the correction coefficients a_c/a versus $1/a$ shows the quick convergence to unity for $a\to\infty$.

path at the opposite edges of the system. Indeed, for a directed polymer on a lattice of $n_b=(L/\xi)$ effective bonds of size $\xi=a^\nu$, the distribution of w converges for $n_b\to\infty$ to a Gaussian with zero mean and standard deviation

$$\sigma_w=C_w\xi(n_b)^\chi, \tag{16}$$

where C_w is a constant. The factor ξ comes from the fact that within each blob, the path is self-similar and thus its transversal deviation scales as the size of the blob ξ. For $L/a^\nu \ll 1$ we have $n_b=1$ and the standard deviation of the transversal deviation scales as

$$\sigma_w=C_wL. \tag{17}$$

From these two limiting behaviors one can conclude that the dimensionless variable σ_w/ξ depends only on the ratio L/ξ, so that $\sigma_w/\xi=F_w(L/\xi)$, where

$$F_w(x) \sim \begin{cases} x, & x \ll 1 \\ x^\chi, & x \gg 1. \end{cases} \tag{18}$$

For large a, percolation theory predicts that $\xi\sim a^\nu$. However, for small a, one can expect deviations from scaling due to discreteness, so it is reasonable to define a parameter a_c such that $\xi=a_c^\nu$, where $a_c(a)/a\to 1$ as $a\to\infty$. This parameter, if it exists, should not depend on L, as we confirm numerically. Thus, taking into account Eqs. (4) and (16) we conclude

$$\sigma_w=C_wL^\chi a_c^{\nu(1-\chi)}. \tag{19}$$

For $d=2$, it is known that $\chi=2/3$ [5], thus $\sigma_w=C_wL^{2/3}a_c^{4/9}$.

To test Eq. (18) we present in Fig. 5(a) the scaled plot of the average absolute value of the deviation $\langle|w|\rangle$. Since the average deviation is equal to zero, we can expect that this quantity scales the same way as σ_w. To achieve good scaling in Figs. 5(a) and 5(b), we select $a_c(a)$ as shown in the inset of Fig. 5(b). The main part of Fig. 5(b) shows the convergence of the distribution of w for large n_b, to the Gaussian limit expected for the directed polymer problem.

[1] D. A. Huse and C. L. Henley, Phys. Rev. Lett. **54**, 2708 (1985); M. Kardar, *ibid.* **55**, 2923 (1985); D. A. Huse, C. L. Henley, and D. S. Fisher, *ibid.* **55**, 2924 (1985).

[2] M. Kardar, G. Parisi, and Y.-C. Zhang, Phys. Rev. Lett. **56**, 889 (1986); M. Kardar and Y.-C. Zhang, *ibid.* **58**, 2087 (1987).

[3] E. Perlsman and M. Schwartz, Europhys. Lett. **17**, 11 (1992);

M. Schwartz, and S. F. Edwards, *ibid.* **20**, 301 (1992); E. Perlsman and M. Schwartz, Physica A **234**, 523 (1996); E. Perlsman and S. Havlin, Phys. Rev. E **63**, 010102 (2001).

[4] T. Halpin-Healy and Y.-C. Zhang, Phys. Rep. **254**, 215 (1995).

[5] A.-L. Barabási and H. E. Stanley, *Fractal Concepts in Surface Growth* (Cambridge University Press, Cambridge, England, 1995).

[6] M. Cieplak, A. Maritan, and J. R. Banavar, Phys. Rev. Lett. **72**, 2320 (1994); **76**, 3754 (1996).

[7] A.-L. Barabási, Phys. Rev. Lett. **76**, 3750 (1996).

[8] P. De Los Rios and Y.-C. Zhang, Phys. Rev. Lett. **81**, 1023 (1998).

[9] N. Schwartz, A. L. Nazaryev, and S. Havlin, Phys. Rev. E **58**, 7642 (1998).

[10] M. Porto, N. Schwartz, S. Havlin, and A. Bunde, Phys. Rev. E **60**, R2448 (1999).

[11] L. A. Braunstein, S. V. Buldyrev, S. Havlin, and H. E. Stanley, Phys. Rev. E **65**, 056128 (2002).

[12] L. A. Braunstein, S. V. Buldyrev, R. Cohen, S. Havlin, and H. E. Stanley, Phys. Rev. Lett. **91**, 168701 (2003).

[13] S. Sreenivasan, T. Kalisky, L. A. Braunstein, S. V. Buldyrev, S. Havlin, and H. E. Stanley, Phys. Rev. E **70**, 046133 (2004).

[14] Y. M. Strelniker, S. Havlin, R. Berkovits, and A. Frydman, Phys. Rev. E **72**, 016121 (2005).

[15] Z. Wu, E. Lopez, S. V. Buldyrev, L. A. Braunstein, S. Havlin, and H. E. Stanley, Phys. Rev. E **71**, 045101(R) (2005).

[16] T. Kalisky, L. A. Braunstein, S. V. Buldyrev, S. Havlin, and H. E. Stanley, Phys. Rev. E **72**, 025102(R) (2005).

[17] W. H. Press, B. P. Flannery, S. A. Teukolsky, and W. T. Vetterling, *Numerical Recipes in C* (Cambridge University Press, Cambridge, England, 2002).

[18] *Fractals and Disordered Systems*, edited by A. Bunde and S. Havlin (Springer-Verlag, Berlin, 1996).

[19] D. Stauffer and A. Aharony, *Introduction to Percolation Theory* (Taylor & Francis, Philadelphia, 1994).

[20] Note that μ_∞ and σ_∞ are not equal to μ and σ defined in (2) and (3).